

# Well Cement Composition Optimization for Deep Well Applications

Guodong Cheng

*School of Petroleum Engineering, China University of Petroleum (East China), Qingdao, P. R. China*

Xueyu Pang (corresponding author; x.pang@upc.edu.cn)

*School of Petroleum Engineering, China University of Petroleum (East China), Qingdao, P. R. China*

Zhengsong Qiu

*School of Petroleum Engineering, China University of Petroleum (East China), Qingdao, P. R. China*

Jiankun Qin

*School of Petroleum Engineering, China University of Petroleum (East China), Qingdao, P. R. China*

Ning Li

*Oil and Gas Engineering Research Institute (Tarim oilfield Company), China National Petroleum Corporation, Tarim, P. R. China*

**ABSTRACT:** Recent studies had revealed that traditional high-temperature resistant silica-enriched well cements are not suitable for deep well cementing applications due to strength retrogression problems in the long term. This study investigated the use of new admixtures, including fly ash and ground blast furnace slag (GBFS), to mitigate such strength retrogression issue of cement. The combined use of GBFS and silica at optimized dosages effectively prevented well cement strength retrogression up to 30d, but strength reduction and permeability increase were still observed from 30d to 90d. On the other hand, the combined use of fly ash and silica effectively prevented both strength reduction and permeability increase of the well cement. However, the addition of fly ash increased the consistency of cement slurry significantly, making it difficult to pump. Finally, the slurries prepared with mixtures of well cement, silica flour, fly ash, and GBFS exhibited both excellent flowability and long-term strength stability.

*Keywords: Fly ash; Granulated Blast Furnace Slag; Silica-enriched well cement; long-term strength retrogression; ultra-high temperature.*

## 1. INTRODUCTION

The development of deep oil and gas reserves as well as geothermal energy brings significant challenges to oil well cement systems due to the high pressure and high temperature (HPHT) downhole conditions. Recent studies have shown that the traditional silica-enriched oil well cement undergoes significant strength retrogression during long-term curing ( $\geq 30$ d) at 200 °C due to microstructure coarsening (Pang et al.,2021). The strength retrogression issue is primarily caused by the fact that deep well cementing requires the cement slurry to set at high temperature conditions, which is in great contrast to many previous studies that focus on low setting temperature and high exposure temperature. This is because many previous studies of high-temperature resistant well cement systems mainly focused on simulating steam injection wells.

During the pumping operation process in deep wells, the cement slurry should remain in a fluid state at HPHT conditions for several hours; after being pumped in place, it finally set and then was directly exposed to HPHT conditions for a long time (Qin et al.,2021). The optimization of silica

admixture (crystallinity, dosage and fineness), increasing curing pressure or adding physical reinforcement materials (such as nanographene and latex fiber) can slow down but not prevent the strength retrogression after a long-term ( $\geq 30$ d) curing period when simulating the deep well cementing condition (Qin et al.,2021; Liu et al.,2021; Qin et al.,2023). Therefore, it is urgent to develop new cementing materials that are applicable to the conditions of deep well cementing.

Fly ash and Granulated Blast Furnace Slag (GBFS) are industrial solid wastes that are recognized internationally as important admixtures for the preparation of high-performance concrete (Teixeira et al.,2022; Liu et al.,2022; Qin et al.,2022; Manojsuburam et al.,2022; Ahmad et al.,2022; San Ha et al.,2022). However, there are little studies about fly ash and GBFS on their performance at high temperature conditions, especially regarding their ability to prevent long-term strength retrogression. In this study, the physical and mechanical properties of well cement blended with silica flour, fly ash and GBFS as anti-strength retrogression admixtures and directly exposed to HPHT curing conditions of 200 °C and 50 MPa are investigated.

## 2. EXPERIMENTAL PROCEDURE

### 2.1 Raw materials

The X-ray fluorescence (XRF) spectrum analysis results of raw materials were shown in Table 1. The Class G well cement and 53  $\mu$ m silica flour were provided by Aksu cement factory and Kuche drilling mud material factory respectively; the GBFS was provided by Beijing Building Materials Science Research Institute Co. Ltd, Beijing, China; the fly ash YFA, fly ash KFA, fly ash SFAI and fly ash SFAII were provided by the same power plant in Shanxi, China; the chemical additives used in cement slurries were the same as those used in our previous studies and were provided by Tianjin PetroChina Boxing Technology Co., Ltd (Pang et al.,2021).

Table 1. Summary of material properties: X-ray fluorescence spectrum (XRF), median size, and density.

Oxide name	YFA	KFA	SFAI	SFAII	GBFS	53 $\mu$ m silica	Class G cement
Al <sub>2</sub> O <sub>3</sub>	38.695	26.589	39.465	39.585	14.12	1.033	2.985
CaO	3.788	5.649	3.330	2.055	43.08	1.452	65.134
Fe <sub>2</sub> O <sub>3</sub>	3.385	7.547	3.138	0.597	0.47	0.866	6.675
TiO <sub>2</sub>	1.820	7.156	1.923	2.167	2.26	0.051	-
K <sub>2</sub> O	0.621	1.294	0.985	0.531	0.34	0.260	0.805
MgO	0.397	0.163	0.855	0.023	6.67	0.399	1.962
Na <sub>2</sub> O	0.097	-	0.138	-	0.28	0.190	0.179
SO <sub>3</sub>	2.604	1.652	2.456	2.155	2.54	0.212	3.15
P <sub>2</sub> O <sub>5</sub>	0.271	2.005	0.274	0.154	0.01	0.023	0.043
SiO <sub>2</sub>	47.994	46.111	47.057	52.548	29.44	95.412	18.452
Free Lime	0.46	0.03	0.03	0.09	0.07	N/A	1.65
D <sub>50</sub> ( $\mu$ m)	18.05	2.47	4.19	4.27	10.67	52.80	14.33
$\rho$ (g/cm <sup>3</sup> )	2.90	2.66	2.64	2.57	2.92	2.67	3.25

### 2.2 Mixture proportion, preparation and test method

The formulation design is presented in Table 2. To avoid breaking hollow particles (cenospheres) that may be present in the fly ash, special mixing methods have to be adopted. During the preparation of slurries m1 to m4 and M1 to M4, the dry blend was added to mixing water and liquid additive in a laboratory blender at a speed of 600 rpm, followed by final mixing at a speed of 3000 rpm for 35 seconds. During the preparation of slurries F1 to F2, the mixed dry material other than fly ash was added to the mixed liquid while stirring at a speed of 4000 rpm and was further stirred at a speed of 12000 rpm for 35s; then fly ash was added as the last component while stirring at a speed of 600 rpm; after fly ash was fully introduced, the slurry was further mixed at a speed of 3000 rpm for 35

seconds. The preparation of slurries without fly ash follows standard API procedures (API 10B-2). The mixing methods should have minimal impact on the property of the slurries as long as they are thoroughly mixed. The compressive strength was measured using a UTM5105X load frame manufactured by Shenzhen SUNS Technology Company. Three replicate specimens were produced for each condition to obtain the average and variability of compressive strength in test result, while two replicate specimens samples in the same batch were used for water permeability tests to obtain the average. Water permeability was measured using a device manufactured by Hai-An Hua Cheng Company, Nantong, China. More details of the above tests can be found in our previous publications(Pang et al.,2021; Qin et al.,2021). The cement slurry thickening time was tested by a HPHT consistometer from Chandler Engineering (Model 8340) at 180 °C and 120 MPa with a ramping time of 50 minutes.

Table 2: Formulation design-dry blend compositions in % by weight of cement (BWOC).

Formulation	cement	fly ash	53 $\mu$ m silica	GBFS	Suspension aid	dispersant	retarder	fluid loss additive	defoamer
C0	100	0	70	0	2.5	0	2.5	6	0.5
S1	100	-	70	20	2.5	5.5	4.5	6	0.5
S2	100	-	70	40	2.5	5.5	4.5	6	0.5
S3	100	-	70	60	2.5	5.5	4.5	6	0.5
S4	100	-	70	80	2.5	5.5	4.5	6	0.5
m1	100	60(YFA)	0	-	2.5	5.5	4.5	6	0.5
m2	100	60(KFA)	0	-	2.5	5.5	4.5	6	0.5
m3	100	60(SFAI)	0	-	2.5	5.5	4.5	6	0.5
m4	100	60(SFAII)	0	-	2.5	5.5	4.5	6	0.5
M1	100	60(YFA)	45	-	2.5	5.5	4.5	6	0.5
M2	100	60(KFA)	45	-	2.5	5.5	4.5	6	0.5
M3	100	60(SFAI)	33.8	-	2.5	5.5	4.5	6	0.5
M4	100	60(SFAII)	33.8	-	2.5	5.5	4.5	6	0.5
F1	100	20(YFA)	75.6	80	2.5	7.5	7.5	6	0.5
F2	100	30(YFA)	67.3	70	2.5	7.5	7.5	6	0.5

### 3. TEST RESULTS

#### 3.1 Compressive strength

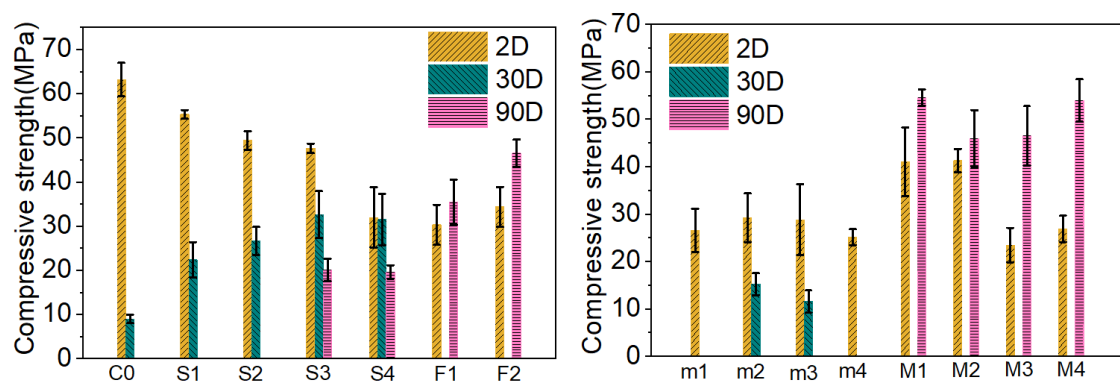


Figure 1. Compressive strength test results of cured slurries at various curing durations.

Figure 1 summarizes the compressive strength test results of cured slurries at various curing durations. The control design slurry C0 consisting of Class G cement and 70% BWOC 53 $\mu$ m silica

experienced severe strength retrogression in the 30 d curing period, with compressive strength declining by 85.83%, confirming our recent studies (Pang et al.,2021). The slurries consisting of Class G cement and fly ash (m2 and m3) saw their strength declined by 48.27% and 60.71%, respectively. The slurries consisting of Class G cement, silica flour and 80% GBFS BWOC showed no strength retrogression within the 30d curing period but still experienced severe strength retrogression during the curing period from 30d to 90d. The slurries containing both fly ash and silica completely prevented the strength decline of well cement systems during the 90 d curing period; the total increase in compressive strength ranged between 11.1% and 101% from 2 d to 90 d curing. It was worth to note that the slurries F1 and F2 containing Class G cement, silica flour, GBFS and fly ash also experienced strength increases; the total increases in compressive strength were 16.67% and 35.30% from 2 d to 90 d curing, respectively.

### 3.2 Water permeability

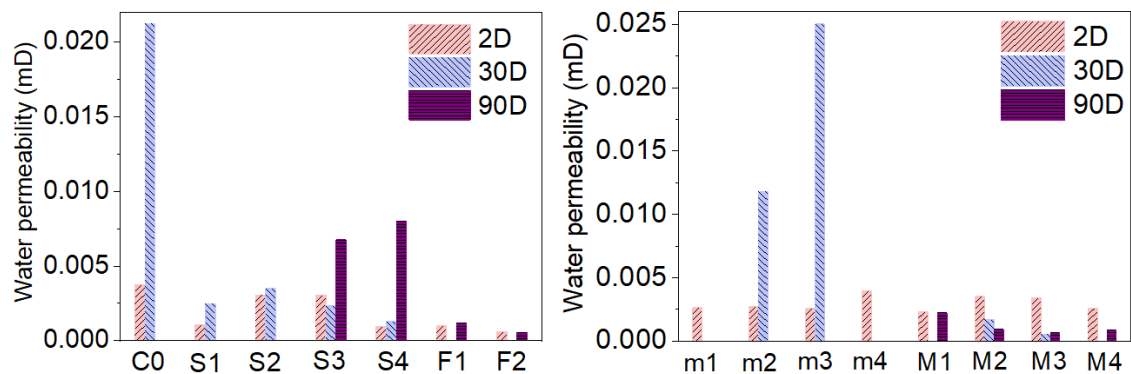


Figure 2. Water permeability test results of set cement at various curing durations.

Figure 2 displays the water permeability test results of set cement at various curing durations. The water permeability of control slurry C0 increased by nearly one order of magnitude (from 0.0038 mD to 0.0212 mD) in the 30d curing period due to microstructure coarsening (i.e., increases in pore size); the use of fly ash alone also cannot prevent permeability increase of the set cement with increasing curing time, while the combined use of fly ash and silica (slurries M1 to M4) effectively reduced the water permeability. Further analysis, smaller fly ash particle sizes (KFA,SFAI,SFAII) seemed to be more beneficial for the stability of water permeability. The addition of GBFS also significantly reduced the water permeability of traditional silica-enriched system; the water permeabilities of slurries S3 and S4 were slightly increased during 90d curing period. It was worth noting that the water permeabilities of slurries F1 and F2 were only 0.001 mD and 0.0005 mD, respectively, after 90d curing period; the total reduction was approximately 72.6% during curing from 2d to 90d.

### 3.3 MIP test results

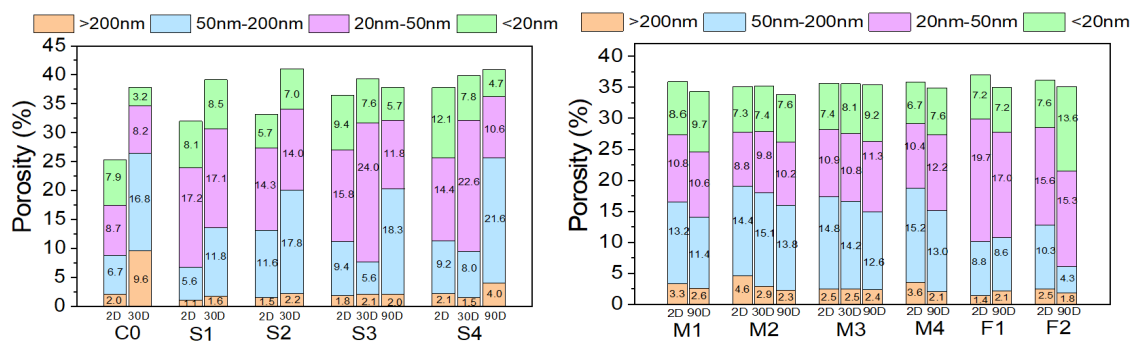


Figure 3. MIP test results of selected slurries at various curing durations.

Figure 3 displays the mercury intrusion test results of selected specimens at various curing durations. The pore structure of cement-based materials was generally divided as follows: harmless pores (<20 nm), less harmful pores (20 nm-50 nm), harmful pores (50 nm-200 nm) and more harmful pores (>200 nm) (Shen et al, 2018). During 2 d to 30 d curing, the total porosity of control slurry C0 increased from 25.3% to 38.0%, where the harmful pores larger than 50 nm increased from 8.7% to 26.5%, indicating that it apparently experienced microstructure coarsening with curing time increasing. The total porosity of slurries containing both GBFS and silica (S1 to S4) were also increased during long term curing period, but the more harmful pores (>200 nm) were reduced. However, the total porosity of slurries containing both fly ash and silica (M1 to M4) showed slight reductions with time; the harmful pores larger than 50 nm were also reduced, while the harmless pores less than 50 nm were slightly increased with time, indicating that the combined use of fly ash and silica effectively prevented microstructure coarsening, consistent with permeability test results. The mercury intrusion test results of slurries F1 and F2 were similar as that of slurries containing both fly ash and silica (M1 to M4).

### 3.4 Thickening time test results

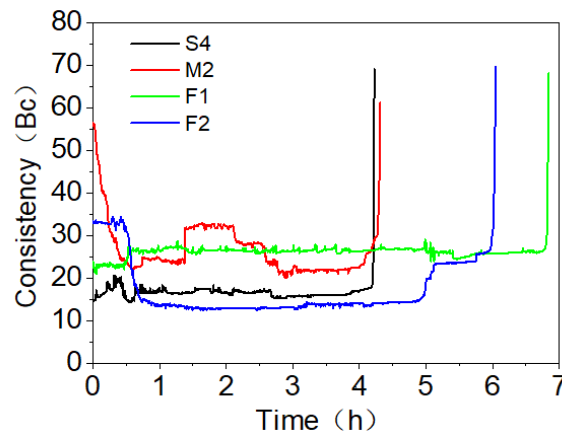


Figure 4. Thickening time test results.

The effects of fly ash and GBFS on the thickening time test results of silica-enriched Class G well cement are presented in Figure 4. The slurry loses pumpability at approximately 70-100Bc. Generally, the slurry consistency is expected to slightly decrease during the temperature ramping period (first 50 minutes) due to thermal thinning effects. However, slurry M2 exhibited unusually high initial consistency and then subsequent fast reduction, which could be due to strong thixotropy (shear thinning) of the slurry; slurry F2 displayed a similar behavior, but the overall consistency was much lower than that of M2. These two slurries also exhibited step increases in consistencies during the thickening time test before final setting of the cement (at approximately 1.5 h for slurry M2 and at 5 h for slurry F2), which indicate abnormal rheological property evolution and may cause complications during cement slurry pumping in field operations. The abnormal consistency evolution profiles of slurries M2 and F2 are likely caused by the addition of high-dosage fly ash. On the other hand, the addition of GBFS appear to be beneficial to the stabilization of rheological properties and led to almost flat consistency evolution profiles before final setting (slurries S4 and F1). The thickening time of slurries S4 and M2 were 258min and 270min, respectively, shorter than that of optimized silica-enriched slurries with total silica dosage in the range of 60-80% (400min-500min) (Pang et al.,2021), possibly due to the fast hydration reaction rate of GBFS and fly ash under hydrothermal conditions. The thickening time can be adjusted by increasing the retarder dosage, as indicated by the test results of slurries F1 and F2. Overall, slurry F1 exhibited best stability and suitable pumping time for filed applications due to the synergistic effects of fly ash and GBFS.

## 4 CONCLUSION

- 1) The addition of GBFS cannot completely stop the long-term strength retrogression of silica-enriched well cement systems at HPHT conditions but can dramatically slow down such process.
- 2) The addition of fly ash in well cement individually cannot prevent the long-term strength retrogression, while the combined use of silica and fly ash can not only stop such process but may also result in gradually improved properties (increases in strength and decreases in permeability) of the set cement during the long-term curing period.
- 3) The addition of fly ash to well cement systems tend to increase the thixotropy of the cement slurry and may lead to abnormal rheological property evolution; fortunately, this phenomenon can be mitigated by further addition of GBFS to the system.

## ACKNOWLEDGEMENTS

This study was founded by China National Natural Science Foundation (No. 51974352 and No. 52288101) as well as from China University of Petroleum (East China) (No. 2018000025 and No. 2019000011).

## REFERENCES

- Ahmad, J., Kontoleon, K.J., Majdi, A., et al. 2022. A comprehensive review on the ground granulated blast furnace slag (GGBS) in concrete production. *Sustainability* 14, pp. 8783. DOI:10.3390/su14148783.
- Guo, J., Dong, M., et al., 2016. Synthesis and property of thermo-thickening oil well cement additives[J]. *Journal of Tianjin University*, 49, pp.597-602. DOI:10.11784/tdxbz201501076.
- Liu, H., Qin, J., Zhou, B., et al. 2022. Effects of Curing Pressure on the Long-Term Strength Retrogression of Oil Well Cement Cured under 200°C. *Energies* 15, pp.6071. DOI:10.3390/en15166071.
- Liu, Z., K. Takasu, H. Koyamada, H. Suyama. 2022. A study on engineering properties and environmental impact of sustainable concrete with fly ash or GGBS. *Constr. Build. Mater* 316, pp. 125776. DOI:10.1016/j.conbuildmat.2021.125776.
- Manojsuburam, R., Sakthivel, E. & Jayanthimani. E. 2022. A study on the mechanical properties of alkali activated ground granulated blast furnace slag and fly ash concrete. *Materials Today: Proceedings* 62, pp. 1761-1764. DOI:10.1016/j.matpr.2021.12.328.
- Pang, X., Qin, J., Sun, L., et al. 2021. Long-term strength retrogression of silica-enriched oil well cement: A comprehensive multi-approach analysis. *Cem. Concr. Res* 144, pp.106424. DOI:10.1016/j.cemconres.2021.106424.
- Qin, D., Dong, C., Zong, Z., et al. 2022. Shrinkage and creep of sustainable self-compacting concrete with recycled concrete aggregates, fly ash, slag, and silica fume. *Journal of Materials in Civil Engineering* 34, pp. 04022236. DOI:10.1016/(ASCE)MT.1943-5533.0004393.
- Qin, J., Pang, X., Cheng, G., et al. 2021. Influences of different admixtures on the properties of oil well cement systems at HPHT conditions. *Cem. Concr. Compos* 123, pp.104202. DOI:10.1016/j.cemconcomp.2021.104202.
- Qin, J., Pang, X., Santra, A., Cheng, G., et al. 2023. Various admixtures to mitigate the long-term strength retrogression of Portland cement cured under high pressure and high temperature conditions. *Journal of Rock Mechanics and Geotechnical Engineering* 15, pp.191-203. DOI:10.1016/j.jrmge.2022.02.005.
- San Ha, N., Marundrury, S.S., Pham, T.M., et al. 2022. Effect of grounded blast furnace slag and rice husk ash on performance of ultra-high-performance concrete (UHPC) subjected to impact loading, *Constr. Build. Mater* 329, pp. 127213. DOI:10.1016/j.conbuildmat.2022.127213.
- Shen, A., Lin, S., Guo, Y., et al., 2018. Relationship between flexural strength and pore structure of pavement concrete under fatigue loads and Freeze-thaw interaction in seasonal frozen regions. *Constr. Build. Mater* 174, pp. 684-692. DOI:10.1016/j.conbuildmat.2018.04.
- Teixeira, E.R., Camões, A. & Branco, F. 2022. Synergetic effect of biomass fly ash on improvement of high-volume coal fly ash concrete properties. *Constr. Build. Mater* 314, pp.125680. DOI:10.1016/j.conbuildmat.2021.125680.